The Astrophysical Journal, 847:119 (6pp), 2017 October 1 https://doi.org/10.3847/1538-4357/aa8872

At a Crossroads: Stellar Streams in the South Galactic Cap

Carl J. Grillmair
IPAC, Mail Code 314-6, Caltech, 1200 E. California Blvd., Pasadena, CA 91125, USA; carl@ipac.caltech.edu
Received 2017 July 28; revised 2017 August 14; accepted 2017 August 22; published 2017 September 28

Abstract

We examine the distribution of old, metal-poor stars in a portion of the recently released PanSTARRs survey. We find an interesting confluence of four new cold stellar stream candidates that appear to converge on or pass near the south Galactic pole. The stream candidates, which we designate as Murrumbidgee, Molonglo, Orinoco, and Kwando, lie at a distance of ≈20 kpc and range in length from 13° to 95°, or about 5 to 33 kpc. The stream candidates are between 100 and 300 pc in width and are estimated to contain between 3000 and 8000 stars each, suggesting progenitors similar to modern day globular clusters. The trajectories of the streams imply orbits that range from hyperbolic to nearly circular. The Molonglo stream is nearly parallel to, at the same distance as, and offset by only $2\overset{\circ}{.}5$ from the previously discovered ATLAS stream, suggesting a possible common origin. Orinoco and Kwando also have similarly shaped, moderately eccentric, obliquely viewed orbits that suggest distinct progenitors within a common, larger parent body.

Key words: Galaxy: halo – Galaxy: stellar content – Galaxy: structure – globular clusters: general

1. Introduction

With the advent of wide-field digital sky surveys, recent years have seen the discovery of several dozen highly collimated, cold stellar debris streams in the Galactic halo (see Grillmair & Carlin 2016 and Smith 2016 for reviews). These streams are clear evidence of the build-up of the halo through the accretion or destruction of ancient star clusters and dwarf galaxies. Moreover, these streams are providing us with sensitive new probes of the Galactic potential and the distribution of dark matter. Analyses of the positions and motions of stars in these streams enable us to constrain both the local and global shape of the potential (e.g., Küpper et al. 2015; Bovy et al. 2016), while the lengths, asymmetries, and discontinuities in the streams can be used to infer the properties of other Galactic components (e.g., Pearson et al. 2017) and of the dark matter itself (Carlberg 2009; Yoon et al. 2011; Carlberg & Grillmair 2013).

Gaia is expected to greatly increase our knowledge of streams and substructures in the halo (Gaia Collaboration et al. 2016). However, *Gaia*'s magnitude cutoff may limit its ability to independently detect the less populous and more far-flung streams. Knowing in advance the locations and trajectories of more distant streams will enable us to both untangle what will no doubt be a very complex data set, and to identify and characterize tracer stars on the red giant or horizontal branches. Accurate proper motions for these tracers would greatly enhance the utility and constraining power of these streams for models of the Galaxy.

While most known streams have been discovered in the Sloan Digital Sky Survey (Abazajian et al. 2009), the recent public release of the Pan-STARRs catalog (PS-1, Chambers et al. 2016) enables us to extend our searches over a significantly larger area of sky. Bernard et al. (2016) recently carried out a survey of PS-1 and, using a matched filter to count stars with colors and magnitudes consistent with an old, metal-poor population, discovered five new stellar debris streams. In this paper, we use a similar technique to more closely examine the region in the south Galactic cap. We describe our detection method in Section 2. We discuss each of our detections in more detail in subsections 2.1 through 2.4. Concluding remarks are given in Section 3.

2. Analysis

We make use of the photometric catalog from data release 1 of PanSTARRs (Chambers et al. 2016). After some experimentation with photometry from the MeanObject and ForcedMeanOject tables, we elected to proceed using the MeanObject table. While this table is less deep than the forced photometry table, we find that in this application the significantly smaller photometric uncertainties in the MeanObject table more than compensate for the somewhat reduced depth. From our experience with Sloan photometry, we elected to download and analyze only the g, r, and i measurements, which are best suited for distinguishing among the relatively blue stars at the main sequence turn-off and below.

To ensure that our sample consisted primarily of stars (as opposed to galaxies), we selected all sources with

$$i_{\rm PSF} - i_{\rm Kron} < -0.307 + 0.0442 i_{\rm PSF} - 0.00777 i_{\rm PSF}^2 + 0.000113 i_{\rm PSF}^3. \quad (1)$$

This is slightly more involved than the simple $i_{\rm PSF} - i_{\rm Kron} < 0.05$ cut suggested by Chambers et al. (2016), but better reflects the locus of stars at faint magnitudes. After some experimentation, we elected to use all stars with $g < 21.8$. Photometry was dereddened using the DIRBE/IRAS dust maps of Schlegel et al. (1998), and corrected using the prescription of Schlafly & Finkbeiner (2011).

We constructed matched filters as described by Rockosi et al. (2002) and Grillmair (2009) using the $g - r$ and $g - i$ distributions of stars in the globular cluster NGC 5053. This cluster has [Fe/H] ≈−2.29 (Harris 1996), yielding filters designed to highlight very low metallicity populations. The luminosity function is modeled as a simple powerlaw, with $N \propto g^{0.3}$. This gives a somewhat greater weight to low mass stars than would a peaked, globular cluster luminosity function, but it accords with our expectations concerning mass segregation in clusters, is consistent with observations of Pal 5's tidal

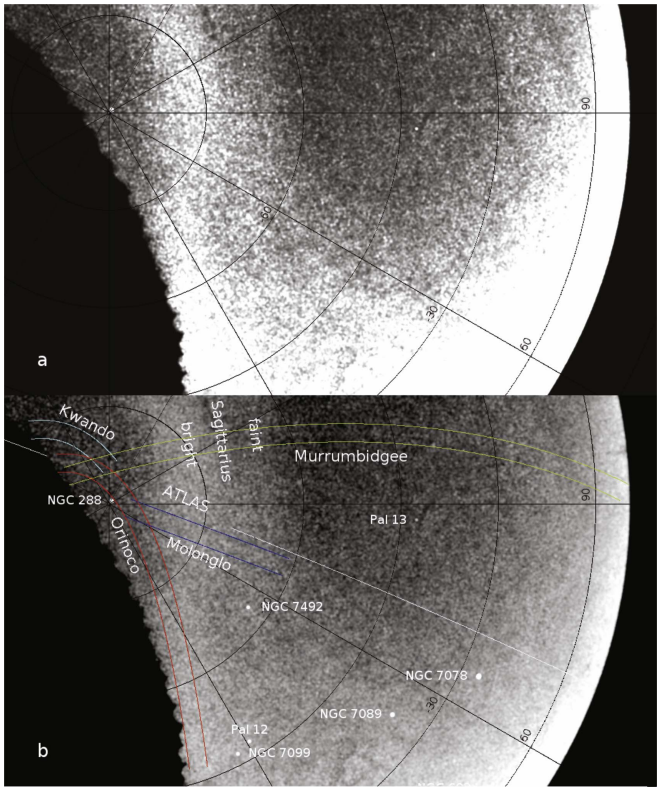

Figure 1. Panel (a): filtered surface density map of the PS-1 survey in the south Galactic cap, smoothed using a Gaussian kernel with $\sigma = 0.^{\circ}4$. The stretch is linear, with brighter areas indicating higher surface densities. Panel (b): the same surface density map with a log stretch, and with streams and nearby globular clusters labeled. The white lines show the great circle fit to the ATLAS stream by Bernard et al. (2016).

tails (Koch et al. 2004) and appears to work quite well. The foreground population was sampled over ≈50% of the area in the south Galactic cap, avoiding regions occupied by the Sagittarius and Triangulum-Pisces streams (Bonaca et al. 2012), as well as various globular clusters in the field. The signal/foreground probabilities computed in each color were then multiplied together before summing the probabilities by position on the sky. We applied the filters to stars in the south Galactic cap after successively shifting the filters in 0.1 mag intervals to distance equivalents ranging from one to 100 kpc.

Figure 1 shows the result of applying our matched filter at a distance of 20 kpc. Five streams are apparent, which all pass within a few degrees of the globular cluster NGC 288 and the south Galactic pole (SGP). The ATLAS stream, first discovered by Koposov et al. (2014) and subsequently extended by Bernard et al. (2016), is easily seen, ending at $\delta \sim -15^{\circ}$. We see no further extensions of ATLAS along the best-fitting great circle determined by Bernard et al. (2016).

Some of the new features in Figure 1 are only barely perceptible, if at all, in Figures 1 and 2 of Bernard et al. (2016). We find that different projections can have a very significant effect on the detectability of very tenuous features, and the streams in Figure 1 (including ATLAS) are much less prominent in either equatorial or Galactic Mercator or Aitoff coordinate projections. We also note that the features in Figure 1 (including the ATLAS stream) largely fade from detectability using a matched filter shifted more than ±0.3 mag from the correct distance modulus for the stream. Moreover, the 20 kpc distance of the features in Figure 1 falls on the

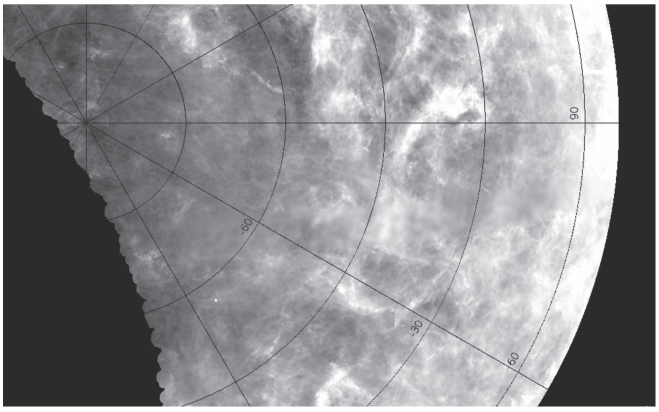

Figure 2. Distribution of $E(B - V)$, as taken from Schlegel et al. (1998), in the same coordinates as Figure 1.

borderline between the intermediate and distant maps generated by Bernard et al. (2016), in effect reducing signal-to-noise ratio at this particular distance, as compared with distances 0.3 mag closer or further away.

Figure 2 shows the distribution of $E(B-V)$ over the same region of sky as in Figure 1 (Schlegel et al. 1998). While we apply a magnitude cut to the sample *after* applying dereddening corrections, inaccuracies in the reddening model could pull in either too few or too many stars from redder and fainter regions of the color–magnitude distribution. However, Figure 2 shows no significant features that can be matched to the lengths and positions of our stream candidates. We conclude that they are not artifacts of reddening-induced completeness variations. We designate the stream candidates as Molonglo, Murrumbidgee, Orinoco, and Kwando. We discuss each of these in turn below.

2.1. Molonglo

The Molonglo stream, detected at the ≈10σ level, is some 22° long, extending from near the globular cluster NGC 288 across both the bright and faint branches of the Sagittarius stream. While pointing almost directly at NGC 288, the stream is at more than twice the 8.8 kpc distance of the cluster (Harris 1996). Moreover, the measured proper motion of NGC 288 (Dinescu et al. 1997) would predict a stream oriented more or less east-west, along the southern limit of the PS1 survey. Molonglo is therefore unlikely to be related to NGC 288.

In equatorial coordinates, the trajectory of Molonglo can be modeled to $\sigma = 0.^{\circ}1$ using

$$\alpha = 345.017 - 0.5843\delta + 0.0182\delta^2 \qquad (2)$$

over the stream extent of $-24.^{\circ}5 < \delta < -12^{\circ}$. The FWHM of the stream is about 30 arcmin. At a distance of 20 kpc, the length and breadth of the stream are therefore 7.7 kpc and 170 pc, respectively. The latter suggests a relatively small or low mass progenitor such as a globular cluster. A background-subtracted, color–magnitude Hess diagram is shown in Figure 3. While obviously contaminated by the Sagittarius stream, Molonglo appears to have a discernible subgiant branch and lower main sequence. As with other streams, shifting the filter brightward or faintward by more than half a magnitude causes the structure to effectively vanish. Estimating the distribution of foreground stars using a heavily smoothed version of Figure 1 and then simply counting stars along the stream within the 3σ color–magnitude envelope yields an

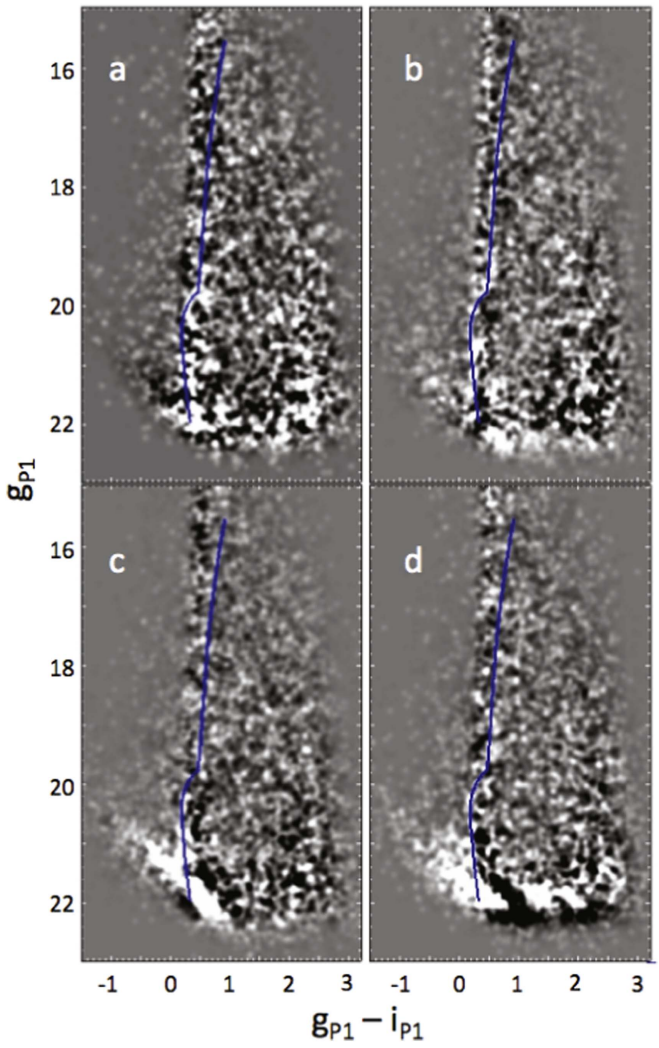

Figure 3. Color–magnitude Hess diagrams of (a) Molonglo, (b) Murrumbidgee, (c) Orinoco, and (d) Kwando. Lighter areas correspond to higher surface densities. The blue curve shows the main-sequence/giant branch locus measured for NGC 5053 and used as the basis of our matched filter, shifted to a distance of 20 kpc. The CMDs of the streams were estimated by generating the CMDs of all stars lying within 0.°25 of each stream and subtracting from these the normalized distributions of stars in selected, much larger fields surrounding each stream. For Murrumbidgee, the CMD was sampled over the region $-65° < b < -30°$, while for Orinoco, we used the eastern 19° of the stream. For Molonglo and Kwando, we used the full lengths of the streams as given in the text.

estimated total of 311 ± 95 stars to $g = 21.8$. Integrating over a globular cluster-like luminosity function then predicts a total of 3700 ± 1100 stars over the 22° length of Molonglo. This is certainly comparable to modern day globular clusters and suggests that Molonglo might once have been a globular cluster itself.

While stars in streams do not precisely follow the same orbits, or the orbits of their progenitors (Eyre & Binney 2011), the observed trajectories of streams can put some constraints on their orbit shapes. These in turn can be used to identify orbit families or possible progenitors. Starting from a designated fiducial point midway along the stream, we use a simple model of the Galaxy with a spherical halo (Allen & Santillan 1991) to integrate a range of possible orbits. Assuming an uncertainty of 0.°2 in the positions of ten normal points evenly spaced along the stream, we use the χ^2 in the positional agreement to arrive at 90% confidence limits for the proper motions and heliocentric velocities at the fiducial point necessary to match the trajectory of the stream. We then push each of these quantities to their 90% limits, integrate the orbits, and choose the extreme cases to put approximate limits on the orbital parameters. These limits are given in Table 1. The best-fitting orbits are shown in Galactic cartesian coordinates in Figure 4.

With no detectable curvature on the sky, the trajectory of Molonglo evidently requires that the progenitor be essentially unbound from the Galaxy. This is somewhat surprising, and one might wonder how the progenitor could have been so extensively disrupted on so benign an orbit. The progenitor must either have been very loosely bound to begin with, or it may have been disrupted by an encounter with some other resident of the Local Group.

2.2. Murrumbidgee

The Murrumbidgee stream is visible (though barely so at its southern end) over the entire field of view in Figure 1, from the SGP to within 5° of the Galactic plane. Using the T-statistic of Grillmair (2009), the portion of the stream with $-65° < b < -30°$ is detected at approximately the 6σ level. The color–magnitude distribution for this portion of the stream is shown in Figure 3 and shows both a weak subgiant branch, along with a somewhat stronger lower main sequence. It also suggests that the stream could be slightly more metal-rich than our adopted search filter. On the other hand, application of a filter based on the color–magnitude distribution of stars in Pal 5 ([Fe/H] = −1.43) yields significantly less signal-to-noise ratio, indicating that the off-locus population at $g \approx 20.6$ in Figure 3 is probably unrelated to the stream.

The trajectory of the stream can be modeled to $\sigma = 0.°14$ using

$$\alpha = 367.893 - 0.4647\delta - 0.00862\delta^2 + 0.000118\delta^3 + 1.2347 \times 10^{-6}\delta^4 - 1.13758 \times 10^{-7}\delta^5. \quad (3)$$

The stream is some 95° long, and some 22 arcmin across (FWHM). At a distance of 20 kpc, these translate to a length of 33 kpc, and a width of 125 pc. The width is again comparable to those of known or presumed globular cluster streams such as Pal 5 (Odenkirchen et al. 2003), NGC 5466 (Belokurov et al. 2006; Grillmair & Johnson 2006), or GD-1 (Grillmair & Dionatos 2006). For the most visible, 45°-long portion of the stream north of the faint Sagittarius stream, subtracting a smoothed foreground distribution and counting stars in the color–magnitude envelope yields a total of 310 ± 120 stars. Doubling this to account for portions of the stream heavily contaminated by the disk or by Sagittarius stream stars, and integrating over a globular cluster-like luminosity function, we arrive at an estimated total of 7400 ± 2900 stars in the visible stream. This is again consistent with a globular cluster progenitor.

Within the limitations of our adopted Galactic model, an orbit fit to Murrumbidgee puts reasonably tight constraints on the orbital plane. The best-fitting orbit is highly inclined and nearly circular, with perigalacticon occurring just north of the faint Sagittarius stream. The orbit passes within 2 kpc of Pal 5 and 3 kpc of NGC 1261. The orbital path of Pal 5 is fairly well described by its tidal tails, and its orbit pole is inclined by more than 30° to that of Murrumbidgee, ruling out any physical

Table 1
Predicted Motions and Orbit Parameters

		Molonglo	Murrumbidgee	Orinoco	Kwando
Fiducial Point	R.A. (°, J2000)	0.163	358.614	359.701	25.025
	Decl. (°, J2000)	−16.869	+16.274	−25.324	−25.107
Prograde Orbit	$v_{\rm hel}$ (km s^{-1})	$+6.1^{+73}_{-329}$	−123 ± 50	+64 ± 3.5	+130 ± 35
	$\mu_\alpha \cos(\delta)$ (mas yr^{-1})	+8.08 ± 0.13	−0.134 ± 0.009	+0.253 ± 0.002	+0.969 ± 0.004
	μ_δ (mas yr^{-1})	−8.15 ± 0.13	+0.388 ± 0.01	−2.28 ± 0.0012	−1.633 ± 0.003
Retrograde Orbit	$v_{\rm hel}$ (km s^{-1})	-118^{+330}_{-73}	−182 ± 50	−121 ± 3.5	−94 ± 35
	$\mu_\alpha \cos(\delta)$ (mas yr^{-1})	−5.91 ± 0.13	+2.152 ± 0.009	+1.91 ± 0.002	+1.865 ± 0.004
	μ_δ (mas yr^{-1})	+3.96 ± 0.12	−3.074 ± 0.011	−2.06 ± 0.001	−2.009 ± 0.003
$R_{\rm apo}$ (kpc)	⋯	>100	24^{+4}_{-1}	21 ± 0.15	$26.4^{+3.2}_{-1.8}$
$R_{\rm peri}$ (kpc)	⋯	20 ± 0.2	$21^{+0.1}_{-2.2}$	6.9 ± 0.1	4.4 ± 0.7
i (°)	⋯	68 ± 1	62 ± 4	79.7 ± 0.1	76.7 ± 4
ϵ	⋯	1 ± 0.3	$0.08^{+0.13}_{-0.001}$	0.5 ± 0.003	0.72 ± 0.02
Orbit Pole	l (°)	193^{+9}_{-2}	160 ± 4	250 ± 0.3	237 ± 15
	b (°)	+22 ± 1	+28 ± 4	+10.3 ± 0.1	+13 ± 4

association. As we have no proper motion information for NGC 1261, we cannot say at this point whether there might be a physical association. If we allow the uncertainties in the fitted proper motions and radial velocities to extend to their 1σ limits, then we find that IC 4499 and NGC 5634 also lie with 3 kpc of an orbit integration.

2.3. Orinoco

The eastern 19° of Orinoco (the portion nearest to the SGP) is detected at the $\approx 15\sigma$ level, and is interesting both for its pronounced curvature and its projected overlap with the ATLAS stream. A portion of the stream appears to be visible in Koposov et al. (2014), though not a length sufficient to have been identified as a separate stream. The western portion of the stream (extending downwards in Figure 1) is much weaker and somewhat conjectural. Fitting an orbit to just the eastern 19° yields a best-fit trajectory that lies alongside and separated by less than a degree from the very faint feature in Figure 1 with $-62° < b < -48°$. Including this faint feature in the fit results in a no less plausible orbit. If indeed the two features are part of the same stream, then it would appear that there is a $\approx 10°$ gap between the two. At this level of significance, it is plausible that this region is simply below our detection threshold. On the other hand, it may also constitute a physical gap in the stream, generated perhaps by a close encounter with a dark matter subhalo or some other Galactic constituent. Finally, we must recognize that this western feature could be an unrelated stream, or not a stream at all.

The easternmost 19° of Orinoco can be modeled to $\sigma = 0.^{\circ}13$ using

$$\delta = -25.5146 + 0.1672\alpha - 0.003827\alpha^2 - 0.0002835\alpha^3 - 5.3133 \times 10^{-6}\alpha^4. \quad (4)$$

This section of the stream has a FWHM of about 40 arcmin, indicating a physical breadth of about 240 pc. This is somewhat broader than the streams above, and may be partly a consequence of confusion with the overlapping ATLAS stream. It may also be indicative of a somewhat more massive progenitor, or more significant or extended heating of the stream (Carlberg 2009). Estimating foreground contamination and counting stars in the appropriate color–magnitude envelope, we find a total of 225 ± 95 stars in the eastern 19° of the stream. Integrating over a globular cluster-like luminosity function, we estimate a total population of 2700 ± 1100 stars.

The eastern (upper) portion of Orinoco apparently bends over and overlaps with a portion of the ATLAS stream (Koposov et al. 2014; Bernard et al. 2016). However, an orbit fit to Orinoco suggests only a few degrees of overlap before the stream diverges from ATLAS in a more southerly direction. We have attempted to fit an orbit to both Orinoco and the southern portion of ATLAS, but the resulting χ^2 is much larger than for either stream alone. We conclude that ATLAS and Orinoco are not different parts of the same stream.

The best-fit orbit for Orinoco passes within 1 kpc of NGC 288, and of NGC 6356. It also passes within 2 kpc of the nearby globulars NGC 6121, NGC 6284, and NGC 6397. From inspection of Figure 1 we know that Orinoco cannot be associated with NGC 288. While the stream appears to arc around the cluster, it does not attach to the cluster in the characteristic "S-shape" we expect (e.g., Pal 5). Using proper motion measurements for the remaining four clusters (Dinescu et al. 1999; Casetti-Dinescu et al. 2010, 2013), we find that all of them have orbits confined to less than 5 kpc vertically from the Galactic disk. The estimated distance of Orinoco (20 ± 3 kpc), combined with the best-fit orbit parameters in Table 1, rule out any association between the stream and these particular clusters.

2.4. Kwando

Faint and not particularly long or continuous, Kwando would not normally have been identified as a stream candidate were it not for its similarity and proximity to Orinoco. The same round-the-pole arc, shifted only a few degrees eastward from Orinoco, was sufficiently striking that we opted to consider it. The stream is detected at the 7σ significance level and, over the range $19° < \alpha < 31°$, the 13° arc of Kwando is

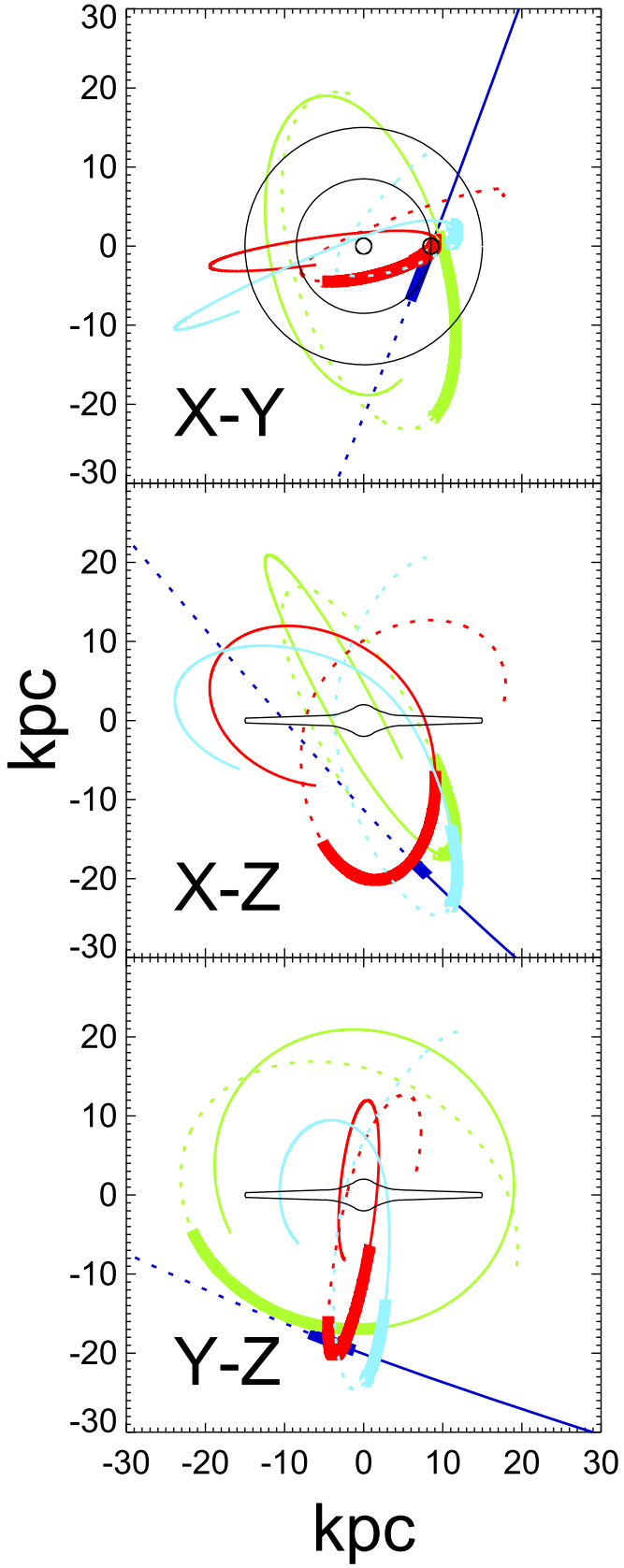

Figure 4. Integrated best-fit orbits, in Galactic cartesian coordinates, for the streams in Figure 1. The position of the Sun and the solar circle are shown in the uppermost panel. The colors are the same as those used in Figure 1. The dotted lines show the forward integrations of the prograde orbits, while the solid lines show the rearward integrations. The thick portions of the orbits are the regions for which we have PS-1 data.

matched to 0°.1 by a polynomial of the form:

$$\delta = -7.817 - 2.354\alpha + 0.1202\alpha^2 - 0.00215\alpha^3. \quad (5)$$

With a FWHM of 22 arcmin, Kwando is evidently only 130 pc across, once again in the realm of presumed globular cluster streams. A color–magnitude selected count of stars yields 120 ± 52 stars over the 13° arc of the stream, or 1400 ± 600 when integrated over a globular cluster-like luminosity function. In terms of linear density, the 9 ± 4 stars per degree actually exceeds the 8 ± 3 stars per degree measured for Murrumbidgee.

As might be expected based on appearance and proximity, the best fit to the orbit of the stream shows fairly similar parameters to that of Orinoco. To within the uncertainties, the inclination and orbit poles are identical. This suggests that, while these streams obviously had distinct progenitors, those progenitors themselves may have formed in the same cloud, or orbited a common parent body.

For Kwando, the best-fit orbit comes within 1 kpc of 47 Tuc. Based on the proper motion measurements of Watkins & van der Marel (2017), an orbit integration for 47 Tuc reveals that the cluster orbit is confined to within 5 kpc of the Galactic plane. A physical association between Kwando and 47 Tuc can therefore be ruled out. Both E 3 and Pal 8 also lie within 1 kpc of Kwando's putative orbit, but neither have published proper motions with which to estimate their orbits.

3. Conclusions

A matched-filter examination of the southern Galactic cap in the PS-1 catalog reveals the existence of four new stellar stream candidates. While Galactic substructures have been detected and mapped in the PS-1 survey area by others (Slater et al. 2014; Bernard et al. 2016; Morganson et al. 2016), we attribute the discovery of these new stream candidates to a matched filter reflecting a more metal-poor population, a different coordinate projection, and perhaps a somewhat finer sampling in distance. Tenuous streams such as these, with of order 10 stars per linear degree, are easily swamped by the much larger number of foreground stars with similar colors. Slight variations in filtering, sampling, projection, foreground estimation, and general technique may be sufficient to either highlight or possibly obscure such streams. The results of this investigation suggest that there may yet be a rich reservoir of cold streams and substructures awaiting discovery in PS-1.

Based on their relatively narrow widths and on memberships estimated between 10^3 and 10^4 stars, we believe the progenitors of these streams to have been globular clusters. They appear to occupy a variety of orbits, from nearly circular to hyperbolic. While a number of existing globular clusters lie near these trajectories, owing to either divergent orbits or lack of proper motion measurements, we find none that can be confidently associated with the new streams. We note that many streams have orbit normals that put them within the region that defines the Vast Polar Structure of Pawlowski et al. (2012). An examination of Table 1 shows that both Molonglo and Murrumbidgee appear to orbit within this plane.

We emphasize that the substructures identified here remain stream candidates until they can be confirmed by radial velocity or proper motion measurements. This will presumably be enabled by the upcoming second *Gaia* data release. Proper motion measurements in particular will in most cases give us much better distances via Galactic parallax (Eyre &

Binney 2009), and ultimately enable more detailed modeling of the Galactic potential.

We are very grateful to B. Shiao and R. White of the Space Telescope Science Institute for their assistance in optimizing PS-1 database queries. We also thank an anonymous referee for several useful recommendations.

The Pan-STARRS1 Surveys (PS1) have been made possible through contributions of the Institute for Astronomy, the University of Hawaii, the Pan-STARRS Project Office, the Max-Planck Society and its participating institutes, the Max Planck Institute for Astronomy, Heidelberg and the Max Planck Institute for Extraterrestrial Physics, Garching, The Johns Hopkins University, Durham University, the University of Edinburgh, Queen's University Belfast, the Harvard-Smithsonian Center for Astrophysics, the Las Cumbres Observatory Global Telescope Network Incorporated, the National Central University of Taiwan, the Space Telescope Science Institute, the National Aeronautics and Space Administration under Grant No. NNX08AR22G issued through the Planetary Science Division of the NASA Science Mission Directorate, the National Science Foundation under Grant No. AST-1238877, the University of Maryland, and Eotvos Lorand University (ELTE).

Facility: PS1.

ORCID iDs

Carl J. Grillmair https://orcid.org/0000-0003-4072-169X

References

Abazajian, J. K., Adelman-McCarthy, J. K., Agueros, M. A., et al. 2009, ApJS, 182, 543
Allen, C., & Santillan, A. 1991, RMxAA, 22, 255
Belokurov, V., Evans, N. W., Irwin, M. J., Hewett, P. C., & Wilkinson, M. I. 2006, ApJ, 637, 29
Bernard, E. J., Ferguson, A. M. N., Schlafly, E. F., et al. 2016, MNRAS, 463, 1759
Bonaca, A., Geha, M., & Kallivayalil, N. 2012, ApJ, 760, 6
Bovy, J., Bahmanyar, A., Fritz, T. K., & Kallivayalil, N. 2016, ApJ, 833, 31
Carlberg, R. G. 2009, ApJ, 705, 223
Carlberg, R. G., & Grillmair, C. J. 2013, ApJ, 768, 171
Casetti-Dinescu, D. I., Girard, T. M., Jilkova, L., et al. 2013, AJ, 146, 33
Casetti-Dinescu, D. I., Girard, T. M., Korchagin, V. I., et al. 2010, AJ, 140, 1282
Chambers, K., Magnier, E. A., Metcalfe, N., et al. 2016, arXiv:1612.05560
Dinescu, D. I., Girard, T. M., van Altena, W. F., Mendez, R. A., & Lopez, C. E. 1997, AJ, 114, 1014
Dinescu, D. I., van Altena, W. F., Girard, T. M., & Lopez, C. E. 1999, AJ, 117, 277
Eyre, A., & Binney, J. 2009, MNRAS, 399, 160
Eyre, A., & Binney, J. 2011, MNRAS, 413, 1852
Gaia Collaboration, Prusti, T., de Bruijne, J. H. J., et al. 2016, A&A, 595, A1
Grillmair, C. J. 2009, ApJ, 693, 1118
Grillmair, C. J., & Carlin, J. L. 2016, in Tidal Streams in the Local Group and Beyond, ed. H. J. Newberg & J. L. Carlin (Berlin: Springer), 87
Grillmair, C. J., & Dionatos, O. 2006, ApJL, 643, 17
Grillmair, C. J., & Johnson, R. 2006, ApJL, 639, L17
Harris, W. E. 1996, AJ, 112, 1487
Koch, A., Grebel, E. K., Odenkirchen, M., Martinez-Delgado, D., & Caldwell, J. A. R. 2004, AJ, 128, 2274
Koposov, S., Irwin, M., Belokurov, V., et al. 2014, MNRAS, 442, 85
Küpper, A. H. W., Balbinot, E., Bonaca, A., et al. 2015, ApJ, 803, 80
Morganson, E., et al. 2016, ApJ, 825, 140
Odenkirchen, M., et al. 2003, AJ, 126, 2385
Pawlowski, M. S., Pflamm-Altenburg, J., & Kroupa, P. 2012, MNRAS, 423, 1109
Pearson, S., Price-Whelan, A. M., & Johnston, K. V. 2017, arXiv:1703.04627
Rockosi, C. M., Odenkirchen, M., Grebel, E. K., et al. 2002, AJ, 124, 349
Schlafly, E. F., & Finkbeiner, D. P. 2011, ApJ, 737, 103
Schlegel, D. J., Finkbeiner, D. P., & Davis, M. 1998, ApJ, 500, 525
Slater, C. T., Bell, E. F., Schlafly, D. F., et al. 2014, ApJ, 791, 9
Smith, M. C. 2016, in Tidal Streams in the Local Group and Beyond, ed. H. J. Newberg & J. L. Carlin (Berlin: Springer), 113
Watkins, L. L., & van der Marel, R. P. 2017, ApJ, 839, 89
Yoon, J. H., Johnston, K. V., & Hogg, D. W. 2011, ApJ, 731, 58